

ACCURATE FREQUENCY TRANSFER BY GPS CARRIER PHASE TECHNIQUE AT CNES

Jérôme DELPORTE, Flavien MERCIER, Michel BRUNET

Centre National d'Etudes Spatiales

18 avenue Edouard Belin - 31401 TOULOUSE Cedex 4 - FRANCE

Phone : 33+5.61.27.44.36 - Fax : 33+5.61.28.26.13 - E-mail : jerome.delporte@cnes.fr

ABSTRACT

The all-in-view GPS carrier phase technique is very promising for accurate frequency transfer. This paper describes the software and the receivers used at CNES Toulouse for frequency transfer using this technique. The software was initially developed by CNES Precise Orbit Determination Group, but it can also be used for ground and space clocks identification.

The Time/Frequency Department uses this software with GPS code and phase data coming from a GPS receiver connected to a Hydrogen Maser. We currently have two GPS receivers : a MiLlennium WAAS (NovAtel) and a Z-12 T (Ashtech). This paper reviews the performance obtained with these two receivers and with two different clock resolution algorithms.

1. INTRODUCTION

For many years, the Global Positioning System (GPS) has been used to compare distant ground clocks. The classical technique is the common-view where the 2 receiver clocks are obtained by processing code measurements on one single GPS satellite (chosen using a predefined schedule). This processing is equivalent to use the single difference code measurement residual at each epoch.

Geodetic GPS receivers are now able to handle several channels (so that several satellites can be observed in the same time) and two frequencies (so that the ionospheric delay can be removed). So, using all the code measurements, an extension of the classical technique is possible in order to have more precise results. Moreover, they are able to record code and carrier phase observables. It is well known that the latter offers promising perspectives for accurate frequency transfer for integration times between several hours and several days [1,2,3].

The aim of this paper is to present the results obtained at CNES using this frequency transfer technique in different configurations. These configurations are described in paragraph 4. The software is described in paragraph 3 and the results are given in paragraph 4.

The originality of this work is clearly the software which is completely independent from other software used for that purpose throughout the world. Our software has two clock resolution algorithms : a least-

mean square method and a Kalman filter approach. The results obtained with these two algorithms are compared.

2. HARDWARE DESCRIPTION

CNES has recently purchased two bifrequency multichannel GPS receivers : a MiLlennium WAAS (NovAtel) and a Z-12 T (Ashtech). The MiLlennium WAAS is a combined GPS/GEO receiver that can be used either with its internal quartz crystal oscillator or with an external clock. The Z-12 T (or Z-12 Metronome) receiver is a modification of the Z-12 for time metrology applications. It uses an external clock instead of an internal oscillator. This external clock shall provide a 20 MHz signal and a 1 pps signal. An appropriate phase between these two input signals shall be applied. The antenna connected to the NovAtel receiver is a GPS - 600 (NovAtel). The antenna connected to the Z-12 T is a choke-ring Ashtech antenna protected by a dome. Both antennas are in open air with no special precaution to control their temperature.

At CNES, the external clock used to feed the GPS receivers is an EFOS B Hydrogen Maser (ON).

3. SOFTWARE DESCRIPTION

3.1. Intercode biases

The GPS dual frequency measurements are used. There are two receiver categories, which give measurements that are not fully compatible. The table below shows what are the Rinex observables, and how they are used :

Receiver	C/A observables	P observables	Phase observables
Ashtech	C1	P1, P2	L1, L2
NovAtel	C1, P2		L1, L2

Table 1 : Receivers' observables in Rinex files

The important observation [4] is that P2 Rinex observable for NovAtel receiver is referenced to C/A code and may be notated as C2 (this measurement can be formulated as $C2 = C1 + (P2 - P1)$). A correction is applied on NovAtel code measurements (intercode biases) in order to have reconstructed measurements P1, P2 compatible with Ashtech.

3.2. Measurement equations

To simplify the equations, the problem is presented without any atmospheric propagation errors.

The measured pseudo-distance is expressed as $P = c \cdot (t_r^{\text{rec}} - t_e^{\text{emi}})$ with c the speed of light, t_r^{rec} is the time of receiver clock at reception event, t_e^{emi} is the time of emitter clock for the corresponding emission event (notation : t_x^y measurement corresponding to event x , in time scale y). The clock offsets relative to GPS reference time scale are h_{rec} for receiver and h_{emi} for GPS satellite. We have $t_r^{\text{rec}} = t_r^{\text{GPS}} + h_{\text{rec}}$ and a similar equation for GPS clock.

We note as $P_{\text{geo}} = c \cdot (t_r^{\text{GPS}} - t_e^{\text{GPS}})$ the 'geometrical' pseudo-distance corresponding to perfect clocks. In the above equations, t_r^{rec} is known, and t_e^{emi} can be reconstructed from the measurements. P_{geo} will be reconstructed using GPS orbits modelisation. Other variables are unknown.

Two formulations are used : a formulation corresponding to a first order expansion of the measurement equations at a reference epoch, and a formulation corresponding to a computation at reception epoch.

3.2.1. Reference time formulation

Here P_{geo} is defined as a function of reception time $P_{\text{geor}}(t_r^{\text{GPS}})$ and is expressed as :

$$P_{\text{geor}}(t_r^{\text{GPS}}) = P_{\text{geor}}(t_0^{\text{GPS}}) + \left(\frac{dP_{\text{geor}}}{dt} \right)_{t_0^{\text{GPS}}} (t_r^{\text{GPS}} - t_0^{\text{GPS}})$$

On the two receivers used in the present study, it is possible to use the value of t_r^{rec} (which are round values) for t_0^{GPS} because the receivers are initialised to have h_{rec} small.

$$P = P_{\text{geor}}(t_0^{\text{GPS}}) + c \cdot ((1 - \alpha)h_{\text{rec}} - h_{\text{emi}})$$

$$\alpha = \frac{1}{c} \left(\frac{dP_{\text{geor}}}{dt} \right)_{t_0^{\text{GPS}}}$$

This formulation is applied at CNES to compute the GPS clocks using a subset of IGS ground stations. These clocks are used for the orbit restitution of a low orbit satellite using GPS measurements. It is interesting, because no a priori knowledge of GPS clocks is necessary.

3.2.2. Measured time formulation

To avoid the α term in the equations, it is necessary to use a reference time sufficiently close to the GPS time of the events. It is possible to use an estimation of the receiver clock (using GPS positioning for example), or directly an estimation of the GPS clocks.

For example, in case of use of an estimation of GPS clocks (\hat{h}_{emi}), P_{geo} is defined as a function of emission time $P_{\text{geo}}(t_e^{\text{GPS}})$ and reference time t_1^{GPS} is an estimation of t_e^{GPS} using a code measurement, for example C1 : $t_1^{\text{GPS}} = t_r^{\text{rec}} - \frac{C1}{c} - \hat{h}_{\text{emi}}$.

$$P = P_{\text{geo}}(t_1^{\text{GPS}}) + c(h_{\text{rec}} - \hat{h}_{\text{emi}})$$

$$t_1^{\text{GPS}} = t_r^{\text{rec}} - \frac{C1}{c} - \hat{h}_{\text{emi}}$$

In the above equation, the error due to the difference between t_1^{GPS} and t_e^{GPS} is of the order of $(t_1^{\text{GPS}} - t_e^{\text{GPS}}) \cdot v$ where v is the GPS satellite velocity. For example, a 300 ns error (~100 meters on C1) in the estimated clock gives less than 2 mm error in the geometry. This means that the formulation is valid even in the case of use of broadcast clocks.

A similar equation can be written for the case of use of an estimation of receiver clock. In this case, the reference time will be a reception time, and function P_{geor} is used.

3.2.3. Remarks

First, rigorously speaking, the two emission times for P1 and P2 signals are not identical, due to ionospheric delays, but this effect is negligible, as the ionospheric delay stays below 100 m for ground stations.

Second, the emission times for the same GPS satellite and two different stations can be different (some 10 ms). The emitter clock is assumed to be unchanged during this period.

3.3. Solution of the equations

The above modelled values are constructed for each station independently, using IGS ephemerides and clocks, satellite attitude and geometry, station ITRF coordinates and centre of phase corrections. The GPS emission time is reconstructed using C1 code measurement.

For the measurements, P1 and P2 are used to obtain the iono free combination (after correction for the NovAtel), and L1 and L2 for the iono free phase combination. A pre-processing procedure applied on each station measurements allows elimination of the wrong code and phase measurements and detection of the cycle slips, without a priori knowledge of the position of emitter and receiver.

Then the partial derivatives relative to station position, clocks (reference time formulation), tropospheric zenith path delay are computed.

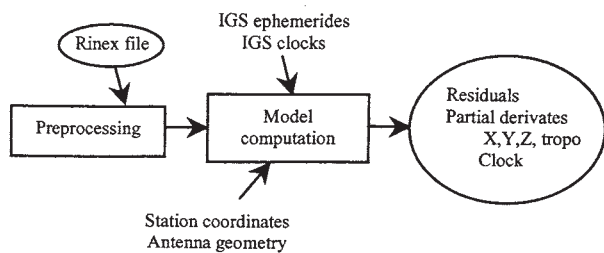


Figure 1 : One station measurement processing

Two filters are then used to obtain the receiver clocks : a least squares filter which allows a resolution on two stations, using single difference measurements, and a global Kalman filter which solves simultaneously for all GPS and receivers clocks. Both filters use code and phase measurements, with adjustment of station coordinates, phase ambiguities and tropospheric zenith path delay. The Kalman filters works on any equation formulation, with possible mixing (case of specific receivers like Aquarius, which measure receiving times of a predefined emission event). The least square filter uses only the second formulation (measured time), in order to produce directly the difference of the station clocks by subtracting the elementary equations.

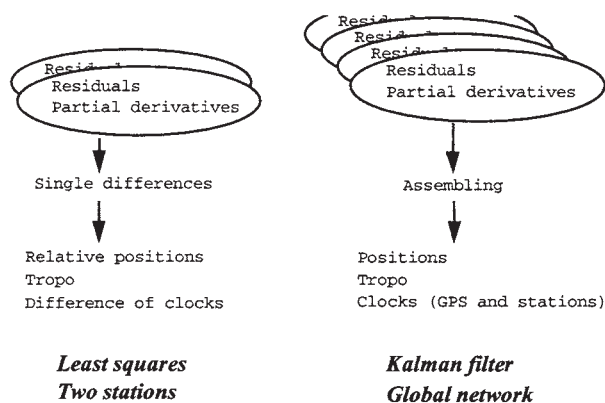


Figure 2 : Resolutions

In the least squares filter, the clocks are eliminated at each epoch, other parameters are solved as global parameters, and the clocks are obtained as the mean of the phase residuals computed using all global parameters only.

In the Kalman filter, all parameters are stochastic (related to a nominal value, for example ITRF values for coordinates), the initial values and covariances and the model covariances used are (30 s sampling values) :

Parameter	Initial value	Initial covariance	Model covariance
Position	0.0	Important	0.0
Position reference	0.0	0.0	0.0
Clocks	0.0	Important	Important
Clock reference	clock bias	0.0	0.0
Tropo	0.0	Small (~0.01 m)	Very small (~1e-5 m)

Table 2 : Parameters of the Kalman filter

4. RESULTS

4.1. Short baseline - Common clock

We performed a frequency transfer between CNES antennas. The baseline is about 1 meter. Both receivers are fed by the Hydrogen Maser. It should allow us to evaluate the intrinsic precision of the phase observable.

We considered a set of 5 consecutive days : days 9 to 13 of year 2002. We have computed the clock solutions with the two algorithms. The figure 5 shows the Kalman filter clock solution (blue) and the least-mean square clock solution (red) :

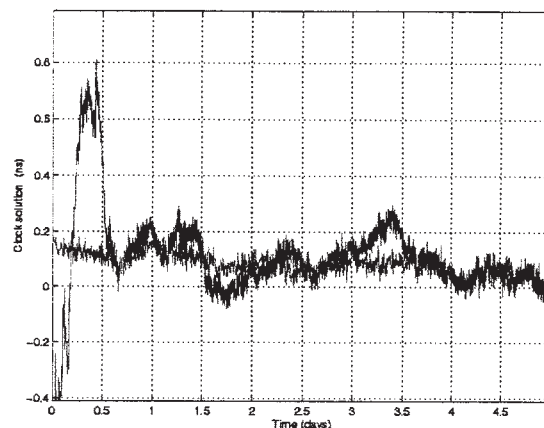


Figure 3 : Clock solutions with the Kalman filter (blue) and the least-mean square (red)

We clearly see the convergence of the Kalman filter at the beginning of the sequence. This convergence duration (about half a day) is due to the identification of the station coordinates and the troposphere correction. It can be minimized by using better a priori values. This convergence duration has been removed for the computation of the Allan deviation. The following figure compares the Allan deviation obtained with the Kalman filter approach (red) and with the least-mean square technique (blue) :

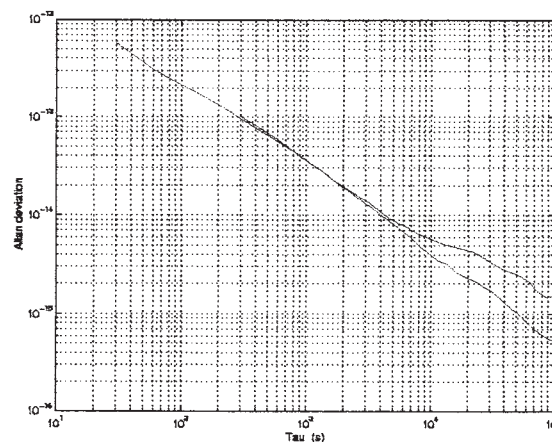


Figure 4 : Allan deviation with Kalman Filter (red) and least-mean squares (blue)

The Allan variance for the Kalman filter results begins to degrade after 10^4 s, which corresponds to the mean pass duration. This has to be investigated further.

With the least-mean square method, we obtain $\sigma_y(\tau) = 4.10^{-15}$ for $\tau = 10^4$ s. This confirms the interest of this carrier phase technique. Yet it should not allow us to characterise Hydrogen Masers for $\tau < 10^4$ s. Although the GPS constellation is less observable, this short-baseline configuration is an optimistic case especially with respect to temperature variations and propagation correction errors (troposphere, geometry, ...).

4.2. Long Baseline : CNES/NovAtel – LPTF/Ashtech

We performed a frequency comparison on 10 consecutive days between CNES and BNM/LPTF Masers. The latter drives an Ashtech Z-12 T which Rinex files are stored on BNM/LPTF web site. The baseline is about 600 km. The figure below shows the result we have obtained with the least-mean square technique :

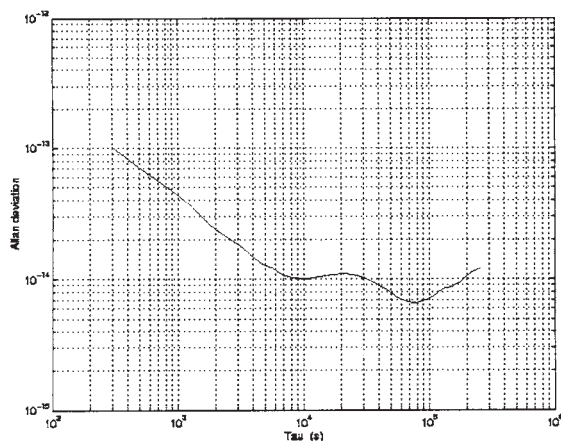


Figure 5 : Allan deviation between CNES/NovAtel and LPTF/Ashtech on 10 days with least-mean squares

For $\tau < 5000$ s, the result is similar to the short baseline result ; this is the resolution noise of the method. For $\tau > 10^5$ s, the result consistent with CNES Maser drift (CNES Maser has no automatic cavity tuning, so it exhibits quite important a drift). Unfortunately, within the interval of interest (that is between 10^4 et 10^5 s), there is a 'bump' that disturbs the frequency comparison. This 'bump' centered at 2.10^4 s has already been observed in previous studies [2,3] with a similar level. We have also observed such a behavior on other long baselines. This 'bump' corresponds to a periodic perturbation with a 12 hours period. The origin of this perturbation is under investigation : temperature variations, mismodelling, ...

4.3. Other Baseline : ALGO/NRC1

The figure 6 shows another frequency comparison between 2 IGS stations equipped with Hydrogen Masers. These stations are ALGO and NRC1 in Canada, the baseline is about 200 km. We performed the

frequency comparison on 5 consecutive days, using the least-mean square method.

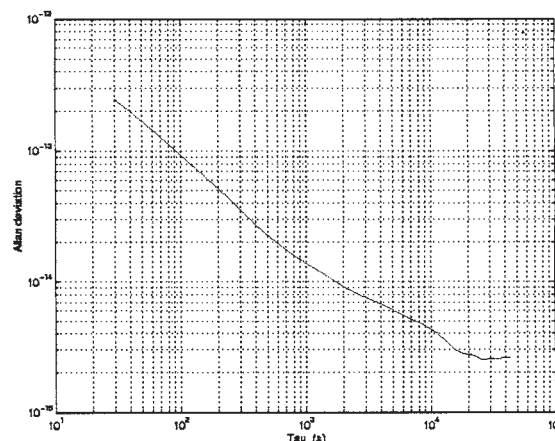


Figure 6 : Allan deviation between ALGO and NRC1 with the least-mean squares technique

This result is quite good and we do not observe the 12 hours petriod perturbation.

5. CONCLUSION

We have evaluated the stability of the frequency transfer by GPS carrier phase in different configurations. We obtain promising results all the more that we did not pay any particular attention to temperature variations. We observed a 12 hours perturbation which origin is still to be investigated.

We have a powerful independent software that includes two different algorithms : a Kalman filter approach and a least-mean square technique. We would be very interested in comparing the clock solutions given by other existing software on the same set of data.

Moreover, we intend to continue this activity with the use of GEO satellites which uninterrupted signal is an interesting point to investigate.

6. ACKNOWLEDGMENTS

The authors would like to thank Mr. Jean-François Dutrey for his essential help in the experimental set-up.

7. REFERENCES

- [Ref. 1] "High Precision Time and Frequency Transfer using GPS phase measurements" - T. Schildknecht, 30th PTTI, 1998.
- [Ref. 2] "Processing strategies for accurate frequency comparison using GPS carrier phase" - G. Petit, EFTF-FCS Joint Meeting, 1999.
- [Ref. 3] "Accurate frequency transfer : progress in the implementation of the GPS carrier phase method at the BNM-LPTF" - F. Taris, EFTF-FCS Joint Meeting, 1999.
- [Ref. 4] Web site of the University of Bern (www.cx.unibe.ch/aiub/ionosphere.html) - see also IGS Mail #2320.